Supersonic molecular beam deposition of pentacene thin films on two Ag(111) surfaces with different step densities

M. F. Danışman
Department of Chemistry, Princeton University, Princeton, New Jersey 08544, USA

L. Casalis
Elettra Synchrotron Laboratory, Trieste, Italy

G. Scoles
Department of Chemistry, Princeton University, Princeton, New Jersey 08544, USA,
International School for Advanced Studies, Trieste, Italy, and Elettra Synchrotron Laboratory, Trieste, Italy
(Received 16 December 2004; revised manuscript received 3 June 2005; published 1 August 2005)

The structure of pentacene thin films grown by supersonic molecular beam deposition on two Ag(111) single-crystal surfaces with different average step distances ($\sim$400 Å and $>$2000 Å) have been studied by low-energy atom diffraction. While the initial stage of the growth is similar on the two different surfaces, regardless of the pentacene kinetic energy and substrate temperature, thicker films show different structural and thermal properties. The ultrathin-film phase has the same structure on both surfaces, showing, however, much larger domain sizes on the substrate with larger average terrace width. In spite of the inferior quality of the ultrathin layer grown on the narrower terraces, upon continuing the growth, a well-ordered multilayer structure is obtained. This, however, occurs in a narrow range of deposition conditions, i.e., at a relatively high kinetic energy of the molecules ($\sim$5 eV) and a low substrate temperature (200 K). On the other, almost ideally flat surface, the order of the pentacene multilayers is, surprisingly, much poorer in spite of the facts that for this surface we have measured an unprecedented 90% of He atom reflectivity and that the measured width of the diffraction peaks of the first monolayer was the narrowest we have ever measured for an organic thin film.

DOI: 10.1103/PhysRevB.72.085404 PACS number(s): 68.55.−a, 68.49.Bc

I. INTRODUCTION

Recently, organic semiconductors have been the object of intense research because of their potential applications in electronic and optoelectronic devices.[1,2] Although organic materials are still far from (and actually are not expected to be) replacing inorganic semiconductors in high-end devices, they are quite promising in applications where flexibility, reduced cost, and easy production are wanted, which cannot be provided by current silicon-based devices. Good examples for this kind of applications are light-emitting diodes (LEDs), flexible displays and their driving circuits, and smart cards.

Pentacene has attracted interest in recent years due to its use in field-effect transistors (FETs).[3,4] Since SiO_2 is the dielectric layer of choice in most FETs, pentacene film growth on silicon substrates and their chemically modified derivatives has been investigated extensively and the film characteristics and the optimum growth parameters on this surface are quite well established at the moment.[5–8] Acene film growth on a variety of metal substrates has also been studied.[9–24] Compared to oxygen- or hydrogen-terminated silicon surfaces, the interaction between organic molecules and metal surfaces is much stronger especially for molecules with reactive groups on metals with unfilled *d*-shell orbitals, which may even lead to dissociative adsorption.[15] For noble metals, however, the situation is more complicated due to weaker interactions, which are, however, stronger than in the case of hydrogen- or oxygen-terminated silicon surfaces, causing a reduced diffusion length and, in turn, poor ordering and relatively small domain sizes. Increasing the surface temperature, in order to facilitate diffusion, increases the domain size and results in Stranski-Krastanov or Volmer-Weber growth, depending on the balance between the molecule-substrate and intermolecular interactions.[13,14,18] Another complication is due to the highly anisotropic nature of the organic molecules, which leads to the formation of polymorphs. In most cases, noble metal surfaces force the molecules of the first layer to lie down flat which, in turn, hinders the formation of ordered overlayers due to lattice mismatch of this first wetting layer with the molecular crystal. However, if the first-layer molecules can adopt a geometry similar to their bulk crystal structure at the expense of some lattice stress or tensile strain, they can form ordered multilayers, which is the case for 3,4,9,10-perylenetetracarboxylic dianhydride on Ag(111).[13,14]

These studies clearly underline the importance of the balance between the substrate-molecule interactions and the intermolecular interactions; while an organic molecule can form a highly ordered film on a substrate at some optimized growth conditions, on another substrate the same parameters may yield a completely different film morphology and structure. The correlation of the effects of the growth parameters provides additional complications. For instance, while increasing the substrate temperature increases the diffusion length, it also activates competing process such as dewetting. The ability to decouple these effects and control the above-mentioned energy balance without tailoring the substrate or

the organic molecule could lead to better films in a much easier way. By using seeded supersonic beams molecules can be accelerated within a certain range and several processes, such as physisorption, chemisorption, or diffusion can be activated without having to raise the substrate temperature. Supersonic molecular beam deposition has actually been used in inorganic semiconductor film growth, and highly ordered films have been obtained at much lower substrate temperatures than usual with a higher growth rate caused by the narrow energy and spatial distribution of the atoms.[25–27] Recently, Iannotta and co-workers have used the same technique for organic film growth on SiO_2 and CaF_2 surfaces, producing films with improved spectroscopic properties,[28,29] hinting at the same time at the presence of improved structural properties. Following these studies and in order to obtain direct structural evidence, in a previous paper we have reported an investigation on the supersonic molecular beam deposition of pentacene films on a "standard" Ag(111) surface with a miscut angle of about 0.6 deg. Using He atom and x-ray diffraction, we were able to show that higher kinetic energies lead to the formation of multilayers of improved structural quality.[30] In the present paper we give a complete account of the previous results and compare them with results from identical studies performed on an Ag(111) surface that had a miscut angle that was so low ($<0.1°$) that only an upper limit could be measured for it. Surprisingly, on this "almost perfect" Ag surface we have not been able to grow, in any growth conditions, good multilayers; therefore we conclude that the presence of steps on "flat" (111) surfaces plays a larger role than previously people believed. While it was known before that a highly stepped surface can act as a template in the growth of different interfacial thin film structures,[11,31] we believe that this is the first time where the influence of *very low* step densities on the growth is studied in great structural detail.

This paper is organized as follows. First an explanation of the He diffraction apparatus and the seeded supersonic source will be given. Then results for the two different substrates will be reported in separate sections, followed by a comparative discussion and conclusions.

II. EXPERIMENT

A. Substrates

While our original intentions were not those of exploring the influence of the surface step density, because of a simple change of crystal we ended up using Ag(111) crystals with very different average terrace widths. The miscut angles of the crystals were determined by measuring the misalignment of the surface normal and the Ag(111) diffraction peak by using x-ray diffraction. The first crystal, which will be referred to as the stepped Ag(111) crystal, has a miscut angle of 0.56° that corresponds to an average terrace width of 380 Å. This in turn results in a specular reflection intensity of the incident helium beam of approximately 30%. The second crystal, which will be referred to as the flat Ag(111) crystal, was almost totally flat since the miscut angle was below the detection limit of our x-ray apparatus, i.e., 0.1°. This surface had a specular reflectivity for the incident helium beam of about 90% that, as far as we know, is the largest atom reflectivity ever measured for a metallic surface. Typical good values for this quantity are in the range of 30% to 50%.

B. Seeded supersonic molecular beam source

The seeded supersonic molecular beam source (SSMBS), described elsewhere in detail,[32] consists of two concentric quartz tubes connected by a hole of diameter ~3 mm. Pentacene molecules are placed at the end of the outer tube which is heated at about 240 °C by means of a tantalum sheet that wraps the tube. The nozzle is further heated with a tantalum wire to keep it from clogging. The temperatures of the nozzle and the body are monitored by two thermocouples that are placed in a shield which covers both the tantalum wire and tantalum sheet. (Due to the unavoidable direct contact of the thermocouples with the tantalum heating material there can be an error of ±20 °C in the recorded temperature values. However, operating at the same source conditions prevents any inconsistencies from run to run.) The heated pentacene molecules diffuse into the inner tube through the hole and mix with the carrier gas. The mixture expands supersonically from the nozzle (100–150 μm and passes to the diffraction chamber through a skimmer of diameter 1 mm). The distance between the skimmer and the nozzle is optimized during the deposition for getting the highest flux. Unfortunately in our setup we cannot directly measure the seeding ratio of pentacene in the carrier gas. But, given the vapor pressure of pentacene at 240 °C [$\sim 3\times10^{-3}$ Torr (Ref. 33)] and the carrier gas pressure of 300 Torr, we do not expect this ratio to be higher than 0.1%.[34] Varying the nature or the pressure of the carrier gas and/or the temperature of the organic material, the average mass of the flowing gas and, as a consequence, the kinetic energy (E_t) of the pentacene molecules can be calculated (including velocity slip corrections) to vary from up to 5 to 0.4 eV by changing the carrier gas from He to Kr.[35]

C. Low-energy atom diffraction

Low-energy atom diffraction (LEAD) measurements were performed *in situ* with a surface scattering apparatus extensively described before,[36] using a monoenergetic He beam with energy of 14 meV (T_{nozzle}=70 K) and $\Delta E/E\sim 2\%$. The reciprocal space of the surface was mapped by detecting the angular distribution of the diffracted atoms at different azimuthal orientations of the substrate crystal. The detector is a liquid-helium-cooled bolometer rotating in the plane that contains the incident beam direction and the normal to the surface. The angle-to-momentum conversion is then performed using the equation $\Delta K_{\parallel}=k_i(\sin\theta_f-\sin\theta_i)$, where $\Delta K_{\parallel}$ is the parallel momentum transfer, k_i is the incident wave vector, and θ_i and θ_f are the incident angle and the detector angular position, respectively. The Ag(111) surfaces were cleaned in UHV by repeated Ar sputtering (1 keV) and annealing (800 K) cycles, until the (0,1) diffraction peak, which defines the Ag(111) $\langle 11-2\rangle$, or next-nearest-neighbor direction, was clearly visible and a specular peak with inten-

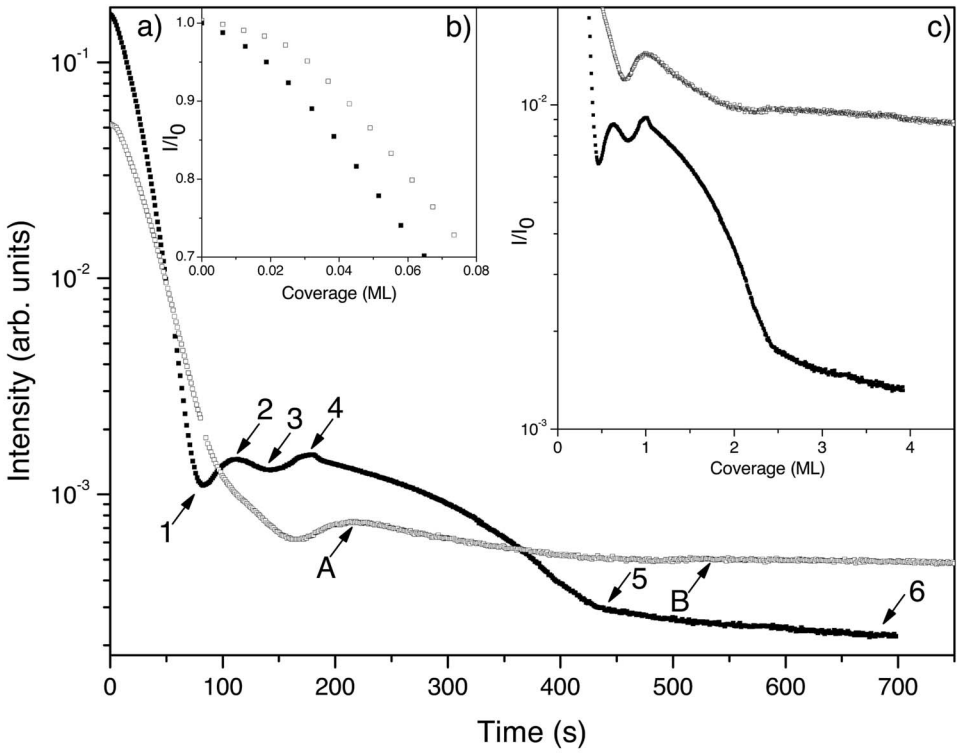

FIG. 1. (a) Specular reflection intensity (relative to incident beam intensity) as a function of pentacene (seeded in helium) deposition time at 200 K substrate temperature from stepped (hollow squares) and flat (solid squares) surfaces. Normalized intensities as a function of coverage are shown in the insets (b) and (c) for the early and later stages of the growth, respectively. Deposition time is converted to coverage by assuming that 1 ML corresponds to point *A* on the stepped surface and to point 4 on the flat one.

sity of at least 25% (for the stepped surface) of the intensity of the primary He beam was detected at the crystal temperature of 80 K).

D. Complementary measurements

Although low-energy atom diffraction is a very useful tool to study the surfaces without inducing any damage, no information related to the internal structure of thick films can be obtained with this technique. To complement the LEAD results and to determine the three-dimensional (3D) structure of the films we have carried out *ex situ* x-ray reflectivity measurements at the beamline X10B of the NSLS at Brookhaven.

III. RESULTS

A. Stepped Ag(111) crystal

1. Structural results

Figure 1 shows He specular reflection intensities as a function of pentacene exposure time, at 200 K substrate temperature and pentacene kinetic energy of ~5 eV (seeded in helium) relative to pentacene deposition on the two Ag(111) surfaces. The decay in the specular intensity that is related to the very large cross section of isolated adsorbates[37] is a function of both surface coverage and growth regime (aggregation, island growth, coalescence, etc.), and can, therefore, be used to characterize the growth dynamics. On the stepped Ag crystal (hollow square curves in Fig. 1), the initial intensity decay [Fig. 1(b)] proceeds in two steps. First there is a slower decay, which we think is an indication of step decoration by the pentacene molecules. The large effective cross section of the adsorbed molecules is in fact reduced by overlap with that of the step edges, which in turn results in slower specular reflectivity decay. Once the steps are saturated, pentacene rafts grow from the steps in parallel with some island nucleation and growth on the terraces, which results in a faster decay followed by a partial recovery. This recovery, which is caused by the overlapping of adsorbate cross sections, can be taken as an indication of completion of the first layer. A second (small) intensity recovery is also visible in the figure around 500 s, pointing to the completion of the second layer. Such oscillations have been observed in metal-on-metal growth studies with recovery peaks almost reaching the initial specular reflectivity values.[38] However, for a film composed of large and soft molecules like pentacene the observed behavior of the intensity is not surprising.

Interrupting the pentacene exposure when a maximum in specular recovery is reached, the diffraction scans along the $\langle 11-2\rangle$ and $\langle 1-10\rangle$ directions were taken. Before the scans, the surface temperature is reduced to below 60 K, in order to minimize inelastic scattering events and to increase the sensitivity of the detector.

Following the diffraction scans, the surface temperature is raised to 200 K again, and pentacene deposition is continued, which resulted in the second, damped, intensity oscillation mentioned above. The diffraction scan taken at this point, resulted in a diffraction pattern completely different from the first layer. This pattern did not change upon further pentacene exposure, apart from the decreasing peak widths. As can be seen in Fig. 2 the first layer (curve *A*) has a 6.1-fold periodicity (with respect to the underlying substrate) along the Ag $\langle 11-2\rangle$ direction;[39] however, no well-resolved diffraction peaks could be observed along other Ag symmetry axes, which prevents a detailed analysis of this initial

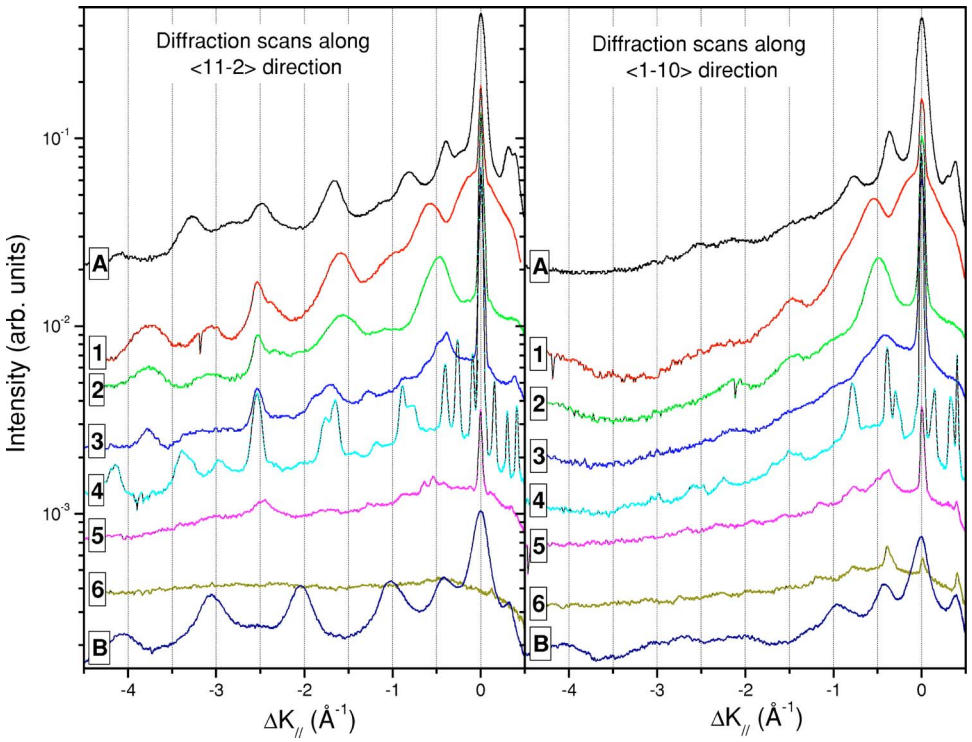

FIG. 2. (Color online) Helium diffraction spectra as a function of pentacene coverage on the stepped and the flat surfaces. Refer to Fig. 1 for notation.

layer. At variance with the first layer, multilayers show diffraction peaks along other Ag symmetry axes (see Fig. 2, curve *B*), which are consistent with a rectangular unit cell of 6.1 ± 0.1 Å $\times 16.5\pm0.6$ Å. After confirming that room-temperature annealing had no effect on the film structure, we performed *ex situ* x-ray reflectivity measurements (data not shown here; see Ref. 30), which gave an interplanar spacing of 3.72 ± 0.01 Å. This value, which is only 5% less than half the *a* spacing (7.9 Å) of the bulk crystal,[40] combined with the LEAD data, results in a unit cell volume that is equal to that of the bulk crystal. Within this unit cell volume, the pentacene molecules can then be placed [by considering the van der Waals dimensions of the molecule and the bulk unit cell structure, as shown in Figs. 3(b) and 3(c)] with the molecular long axis tilted 20° with respect to the Ag(111) $\langle 1-10\rangle$ direction, and with the layers stacked in a herringbone fashion. This film structure resembles a bulk crystal placed on its *b*-*c* plane [$b=6.06$ Å, $c=16.01$ Å (Ref. 40)] on the surface. Although it is also possible to arrange the molecules in slightly different ways in the unit cell, since we do not have sufficient experimental information to determine the true molecular arrangement we discussed the proposed structure as a starting point as it retains the molecular arrangement of the bulk. The asymmetry in the x-ray reflectivity peak not only confirms that the first layer has a different structure from the multilayer but also indicates that the molecules are lying down flat on the Ag surface. The best fit to this peak is obtained by placing a flat pentacene layer at the interface with a distance of 7.8 Å between the silver surface and the first tilted pentacene layer.

2. Effect on the growth of substrate temperature (T_s) and kinetic energy (E_i)

After characterizing the film structure we studied the effect of substrate temperature and the kinetic energy on film growth. The results summarized in Fig. 4 indicate that the kinetic energy does not affect the interface layer structure. However, the substrate temperature has a slight influence on the domain size, which reaches its largest dimensions,

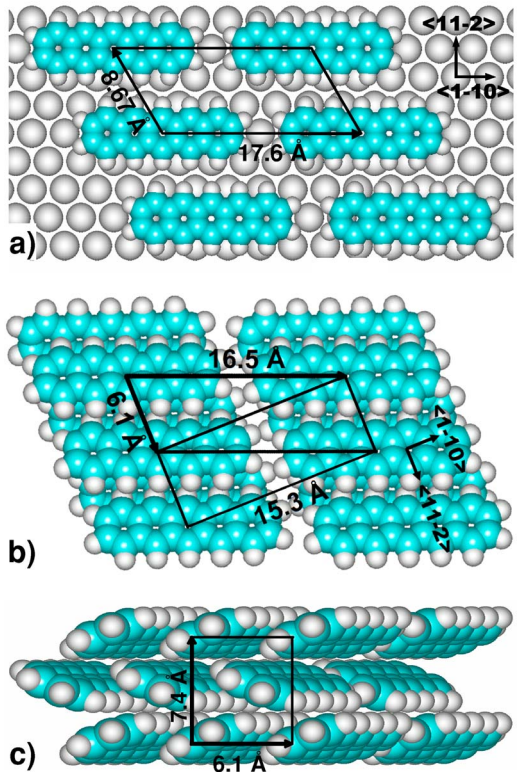

FIG. 3. (Color online) Structural model of the film: (a) top view of the monolayer, (b) top view of the multilayer, and (c) side view of the multilayer.

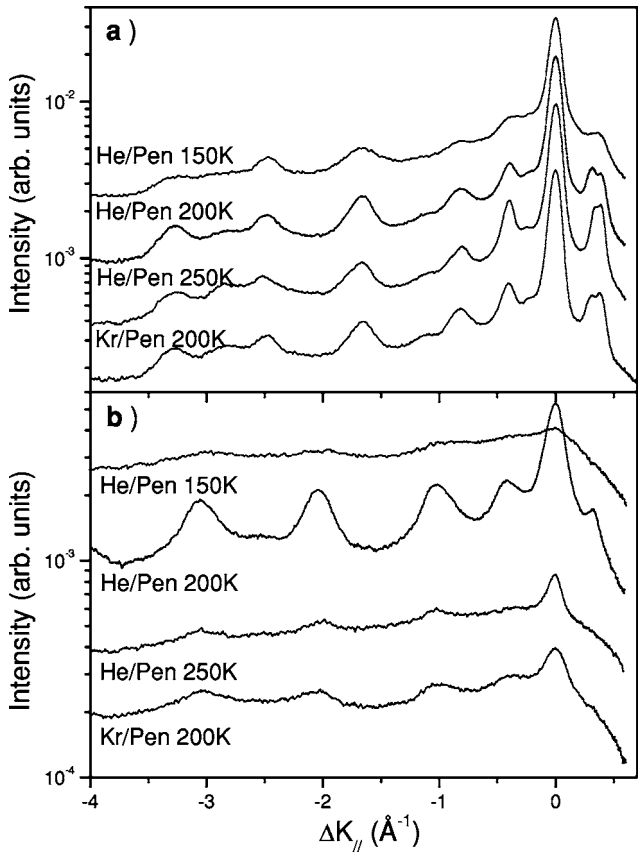

FIG. 4. First-layer (a) and multilayer (b) structure as a function of substrate temperature and kinetic energy on the stepped surface.

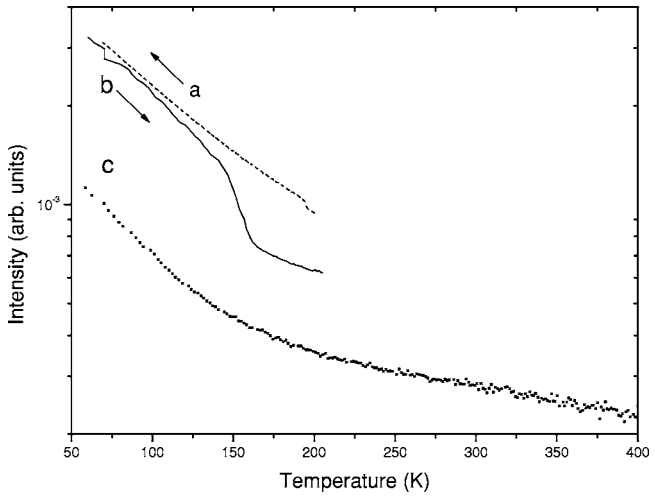

FIG. 5. Thermal traces from different film phases on the stepped surface recorded during cooling first layer (a), heating first layer (b), and heating multilayer (c).

though still smaller than the transfer width of the diffraction apparatus, below 200 K. The effect of substrate temperature on the film growth is more visible in the multilayer structures, the best of which can be obtained at 200 K [Fig. 4(b)]. At higher or lower temperatures diffraction peaks get broader and the specular intensity decreases substantially, indicating a smaller average domain size and a rougher surface. Although annealing to 300 K resulted in improvement in peak widths and specular intensities, these never reached the values of the films grown at 200 K. Low-kinetic-energy deposition also resulted in poor multilayer quality, suggesting that the kinetic energy is key to improving film quality. We will return to this point in the following sections: here, we should note that in both cases, low-temperature (150 K) and low-energy depositions, the fluxes were somewhat (2 to 4 times) lower than for 200 and 250 K depositions. Although different fluxes could be responsible for the differences in film quality one would expect the low deposition rate to favor a better film growth,[3,6] which is contrary to our observation.

3. The thermal stability of the films

The specular reflection intensity recorded during heating and cooling the films is shown in Fig. 5. The films, grown by either high- or low-kinetic-energy deposition, showed the same thermal behavior until desorption of the multilayer; therefore in Fig. 5 only data from the high-kinetic-energy deposition films are shown. Curve *a* was obtained during cooling of the first layer just after deposition at 200 K. When the same surface was heated, however (curve *b*), a sharp decay in specularity was observed at about 145 K, which is probably due to a phase transition. We note that for all the other cases the traces recorded in either direction were almost the same. The initial decay of the multilayer heating trace (curve *c*) had the same slope as that of the first layer up to about 160 K; from there on, however, a slower decay was observed, which is probably due to annealing of defects and the desorption of the multilayer around 400 K. Although a multilayer desorption peak could not be detected due to similar surface roughness and stiffness of the first layer and the multilayer, we still were able to deduce a desorption energy range of 1.14–1.24 eV (by considering the annealing temperature range in which, the multilayer diffraction pattern degraded considerably).

B. Flat Ag(111) crystal

1. Structural results

We studied the flat Ag crystal in the same way as the stepped one. In Fig. 1, a comparison of the specular reflectivity of the two crystal surfaces shows big differences in behavior. First, the initial slow decay is almost missing for the flat surface (solid squares curves), which supports the thesis of step saturation. Another difference is the observation of two consequent recovery peaks for the flat surface, the second of which may be due to a phase transition or completion of a second layer. After the second recovery, the flat surface shows a sharp decay stabilizing at a reflectivity value that is much lower than that of the stepped surface, which points to the growth of a disordered multilayer phase.

As in the case of the stepped crystal we stopped at different positions along the specular reflectivity decay curve (indicated as 1,2,…,6 in Fig. 1) and checked the structure of the film (see Fig. 2). Structures 1 and 2 are identical except for the positions of very broad peaks around the specular peak. These peaks are probably due to the rows of pentacene with

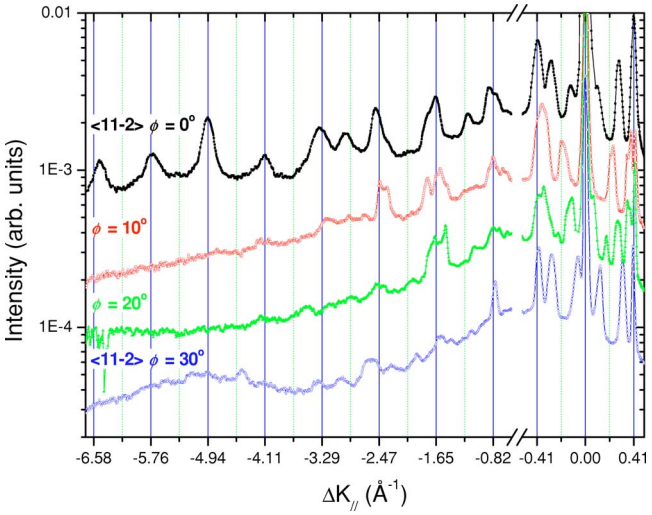

FIG. 6. (Color online) Diffraction scans of structure 4 taken along four different azimuthal angles. The region between −0.5 and 0.5 $Å^{-1}$ is expanded for the sake of clarity. Grid lines indicate the expected peak positions for one domain of the 6.1×3 unit cell. When the remaining five rotational and mirror domains are considered the mismatch between some of the grid line and peak positions can be accounted for.

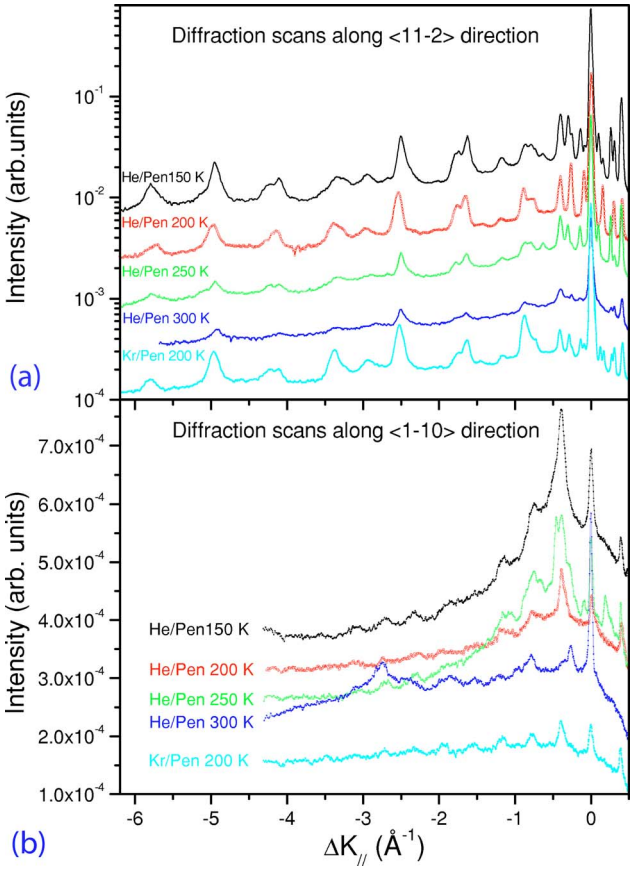

FIG. 7. (Color online) (a) Diffraction pattern of 4 as a function of substrate temperature and kinetic energy. (b) Multilayer structure as a function of substrate temperature and kinetic energy.

decreasing inter-row spacing as the coverage increases. Structure 3 is a transition between 2 and 4, which can clearly be seen in both Figs. 1 and 2. One can easily notice that 4 has the same periodicity as the first-layer structure formed on the stepped Ag crystal (curve *A* in Fig. 2). However, the peaks are much narrower and limited only by the instrumental resolution in the case of flat Ag crystal. Surprisingly no diffraction pattern could be observed from the multilayer along the $\langle 11-2\rangle$ direction on the flat substrate even though the interface layers were much better resolved. Along the $\langle 1-10\rangle$ direction, though, peaks with a periodicity of 16.1 Å could be observed. The fact that the multilayer has completely different diffraction patterns on different substrates even though the interface layers were very similar will be discussed in the following sections.

Some representative diffraction scans along several azimuthal directions of structure 4 are shown in Fig. 6. All the peak positions can be reproduced by assuming a 6.1×3 unit cell of lying-down pentacene molecules [Fig. 3(a)]. Close-coupling calculations also agree quite well with the peak intensities for small $\Delta K_{\|}$ values; however, due to the limitations of the code we are using, the peak intensities far from the specular could not be reproduced well and currently we are in the process of modifying the code in order to get a better fit.[41] Lastly we should note that the peaks that appear between ±0.41 $Å^{-1}$ and the specular peak are off-azimuth peaks which appear due to the geometry of our detector which has a broad slit perpendicular to the scattering plane.

2. Effect on the growth of T_s and E_i

Since 4 was the best-resolved structure that we could obtain, we studied the effect of substrate temperature and the kinetic energy of the molecules being deposited on this structure along with the multilayer. The results are summarized in Fig. 7. When the film is grown at substrate temperatures higher than 200 K, both interface-layer and multilayer diffraction peaks get broader. Above 250 K, however, the specular intensity of the multilayer film increases and the diffraction pattern shows no periodic structure. As in the case of the stepped silver surface, the first layer did not show much dependence on the kinetic energy. The diffraction pattern of the multilayer, however, did not change as a function of kinetic energy on the flat silver substrate, contrary to the case of the stepped silver surface.

3. The thermal stability of the films

Due to the above-mentioned similar characteristics of films grown by either high- or low-kinetic-energy deposition we studied the thermal stability of the films only for the case of high-kinetic-energy deposition (see Fig. 8). Structure 4 (dashed line) has a slightly higher decay rate than 2 (solid line), and unlike the first layer grown on the stepped surface, did not show any phase transition during heating. The multilayer, on the other hand, showed no temperature dependence, probably due to its rough surface, which results in very low specular intensity levels slightly above the diffuse scattering background. This, however, also made the observation of a specular intensity rise due to desorption much easier, since the underlying substrate and/or interface layers

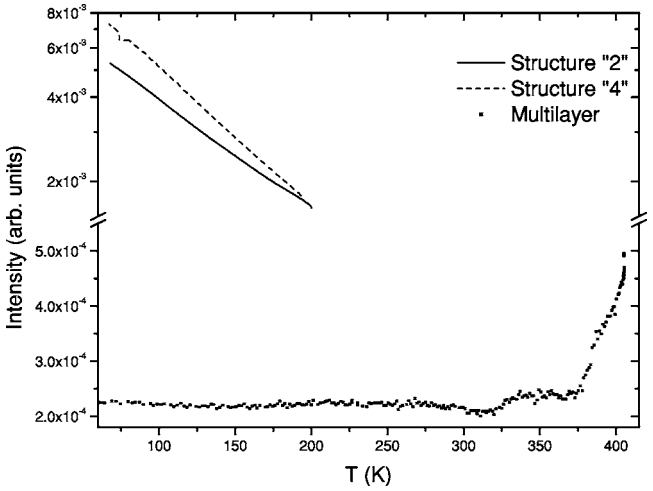

FIG. 8. Thermal traces of different film phases on the flat surface. For detailed explanation see text.

had a much higher specular intensity. Two such intensity rises could be seen in the heating trace of a multilayer grown by high-kinetic-energy deposition (■ symbols), with the lower-temperature one having smaller amplitude. This amplitude difference can be explained by the different roughness of the underlying layers remaining on the surface after desorption. The low-temperature rise at 328 K corresponds to a desorption energy of 0.97 eV and the higher-temperature one at 382 K corresponds to 1.13 eV.

IV. DISCUSSION

A. Initial growth

Even though the specular reflectivity vs time of exposure decays in a different fashion for different surfaces (two specular recovery points observed on the flat surface as opposed to one on the miscut crystal), the fact that the diffraction patterns from the first-layer film on the miscut surface and structure 4 on the flat surface are identical suggests that up to this point film growth follows a similar path on both surfaces. The smaller terrace width of the miscut surface, which yields smaller domain size films, may be the reason for the missing (or unresolved) first specular recovery on this surface. Due to this fact, the discussion on the nature of the interface layer phases will mainly be based on the results obtained on the flat surface, whereas discussion on the growth mechanism will be focused on the effect of the steps.

1. Growth mechanism

As mentioned before we think that step decoration causes the slow specular reflectivity decay during the very early stages of deposition. The inset of Fig. 1 shows a comparison of the normalized deposition curves for the stepped and the flat silver surfaces. Clearly the initial slow decay is missing in the case of the flat surface. Such step decoration has been reported by several groups in the past. Lukas *et al.* have reported preferential binding of naphthalene and anthracene to the step sites on vicinal Cu(111) surfaces with a binding energy 0.15 eV larger than that of the terrace sites.[11] A similar selective binding to the step edges has also been observed during the growth of PTCDA films on Ag(111) (Ref. 31) and pentacene on Cu(119).[23]

2. Low-coverage phases

In this section we will focus on the low-coverage film phases (Fig. 2, spectra 1 and 2) and in the light of previous results obtained on different substrates we will try to explain our own results. Several low-coverage pentacene film phases have been observed recently both on Au(111) surface by France *et al.*[9] and on Ag/Si(111)-$(\sqrt{3}\times\sqrt{3})R30°$ surface by Guaino *et al.*[20] France *et al.* have reported low-coverage unit cells with inter-row spacing ranging from 32.4 Å [for 0.3 monolayer (ML)] to 15.3 Å (for 1 ML). For very low coverage (0.3 ML) the rows were made up of head-to-head pentacene molecules, whereas for higher coverage (1 ML) molecules are aligned side to side in the rows. On the Ag/Si(111)-$(\sqrt{3}\times\sqrt{3})R30°$ surface at 0.35 ML coverage pentacene molecules formed head-to-head rows with an inter-row spacing of 15.8±2 Å. For still lower coverages (0.2 ML), although molecules retained their head-to-head organization, the inter-row spacings were much larger and equal to multiples of the substrate unit cell length (6.8 Å$\times$2.5, $\times$5, $\times$6.5). From these studies it can be concluded that pentacene molecules align head to head or side to side in a row as a function of coverage, and the distance between these rows changes with coverage. When the spectra 1 and 2 in Fig. 2 are examined two kinds of diffraction peaks can be noticed; the very broad peaks around the specular region and the ones after -1 Å^{-1}. The latter kind of peaks can pretty well be described with a periodicity of 0.34 Å^{-1} which corresponds to 18.5 Å and show up only along the $\langle 11-2\rangle$ direction. This may be due to chain of molecules running along $\langle 11-2\rangle$ axis, composed of head-to-head pentacene molecules. The second kind of peaks may be due to quasirandom distribution of inter-row distances around a certain value (as large as 60 Å), which results in very broad diffraction peaks very close to the specular peak position (and due to the poor azimuthal resolution of the instrument at small $\Delta K_{\|}$ values these peaks appear along all azimuthal directions). While the head-to-head configuration of the molecules inside the rows does not change as the coverage increases from 1 to 2, the most probable inter-row spacing may be decreasing, causing the first kind of diffraction peaks to drift away from the specular position.

3. Full-coverage phase

Structure 4 can be either a second layer or a different monolayer structure with a packing denser than 2. Although it is quite difficult to be sure, we think the latter possibility is more probable, and below we will try to justify this hypothesis.

The first thing we should consider is the domain size and the ordering of these two films. As mentioned before, 4 has slightly higher specular reflection intensity and much sharper diffraction peaks, which is consistent with a monolayer structure with larger domains. Next, we would like to turn to

Fig. 1(c), where specular reflection intensity as a function of coverage is plotted, assuming 4 corresponds to one monolayer. Based on the previously mentioned unit cell dimensions, the lateral packing density ratio of the multilayer (on the stepped surface) and structure 4 can be calculated as 1.4. Assuming a constant sticking coefficient (as a function of film thickness), and that 4 corresponds to a monolayer coverage, this value necessitates about 2.4 ML deposition for the completion of the second layer. In Fig. 1(c), in fact, a second damped oscillation can be observed for the stepped surface at around this coverage value. On the flat surface, again after 2.4 ML deposition, the sharp decay in the specular intensity comes to an end, which may be a signature of the completion of the transition from the monolayer to the second layer.

However, even though we believe 4 is a monolayer structure, we cannot exclude the probability of its being a second layer. In fact, formation of metastable second- and higher-level films beneath the stable bulklike films have been observed before, during the growth of pentacene on Cu(110) (Ref. 16) and pentacene on Ag(111) (Ref. 42) and Fig. 8 may be a signature of this.

B. Multilayer

1. Growth mechanism

We believe the crucial step for the formation of an ordered multilayer structure is the transition from the monolayer to the multilayer. For the stepped silver surface the specular reflection intensity of the monolayer and the multilayer are very close to each other. Also the softness of the monolayer and the multilayer is almost the same. However, in the case of a flat surface a sharp decay in the specular reflection intensity takes place after the completion of a monolayer which ends up at a value almost an order of magnitude less than the monolayer. Actually this value is very close to the limit of diffuse scattering, and does not show any temperature dependence, which indicates a very rough surface.

Pentacene molecules in the monolayer have a lying-down arrangement, which does not match any of the planes of the bulk crystal. As a result, in order to form a multilayer film, the molecules deposited on this smooth monolayer should either force the monolayer film to rearrange to a structure that resembles the bulk symmetry or form a second layer at the expense of lattice mismatch. Due to relatively strong interaction of the pentacene molecules with the silver substrate we believe that the former process is not taking place in our case. Actually in all the previous studies about pentacene on Cu, Ag, and Au, a lying-down monolayer structure is observed. Lastly the asymmetry in our x-ray data is also consistent with a lying-down initial layer. This leaves us with the tilting scenario which is actually observed during pentacene film growth on Si (Ref. 7) and Cu (Ref. 16) surfaces previously. Similar to what is observed on Cu(110) we too observed a lying-down monolayer covered with tilted second-layer molecules. However, in our case the directionality provided by the monolayer is missing due to smoother corrugation potential and higher symmetry of the Ag(111) surface [than that of Cu(110)] which in turn results in a less corrugated monolayer structure with six equivalent domains. These would make the nucleation of a tilted second layer much more difficult on the flat Ag(111) surface. In the case of the stepped Ag(111) surface on the other hand, we think that step edges act as nucleation sites for the tilted molecules and initiate a step flow growth which in turn results in an almost constant specular reflection intensity after the completion of a second layer. Since this extra dimensionality is missing for the flat Ag(111) surface, even the extra kinetic energy provided by supersonic deposition cannot initiate the growth of an ordered second layer, which in turn results in a sharp specular reflectivity decay. But still the overlayer manages to follow the symmetry of the underlying monolayer phase to some extent. In Fig. 2 it can clearly be seen that during the transition from the monolayer to the multilayer (from 4 to 6) the periodicity along $\langle 11-2\rangle$ direction diminishes completely whereas along the $\langle 1-10\rangle$ direction the peaks shift only 0.2 Å^{-1}.

2. Effect of kinetic energy on the film growth

We believe the extra kinetic energy provided by supersonic deposition enhances the diffusion length of the molecules on the surface and makes the formation of ordered films possible at relatively low substrate temperatures, where competing processes such as dewetting or formation of different polymorphs are suppressed. Quasi-layer-by-layer growth at low substrate temperatures (up to 70 K) has been observed by reflection high-energy electron diffraction (RHEED) (Ref. 43) and LEAD (Ref. 44) for homoepitaxial metal systems. Since at 70 *K* thermally activated diffusion is not relevant the RHEED results were attributed to a diffusion mechanism driven by the energy gained by the adatoms from the latent heat of condensation. It is then reasonable to expect a need for an extra amount of energy in the case of organic molecular films, in order to activate a layer-by-layer type of growth, since the heat of condensation is lower then metals, and the crystallization involves more complex rearrangements[45] in the latter case. Therefore, we think that, on the stepped surface, a step flow growth takes place after the completion of the second layer, and since the substrate temperature is low, processes such as 3D islanding[13,14,18] or the nucleation of the bulk phases on a thin metastable multilayer film[16] are suppressed.

V. CONCLUSION

We have reported the formation of ordered thin films on two Ag(111) substrates with different step densities. On both surfaces identical monolayer structures have been observed. While the steps limit the domain size of the monolayer film on the miscut surface, they also initiate the growth of an ordered multilayer film with a unit cell that is very similar to the *b-c* plane of the bulk crystal. On the flat surface, although the average monolayer domain size was much larger, no ordered multilayer film structure could be observed. Even though we suspect that the presence of a larger number of steps may be responsible for the improved growth conditions on the "worst" of the two substrates, since the phenomenon occurs in a rather narrow range of growth parameters, it is

not excluded that in an even narrower region of this parameter space also the well-ordered substrate may allow for the growth of a well-ordered multilayer. Since, however, in spite of a very extensive search, we have failed in finding such a happy set of growth conditions, we are forced to conclude that further work is necessary in which the step density is changed more gradually than was done, serendipitously, in the present work. The monolayer was found to be metastable on both surfaces and after a 400 K annealing of the multilayer films different lower-coverage monolayer phases have been observed on different substrates. On both surfaces the optimum growth temperature was 200 K and higher substrate temperature caused disordering. While local annealing induced by the impact of high-energy pentacene molecules has a decisive role in improving the growth on the miscut surface, no appreciable effects were observed on the flat surface.

ACKNOWLEDGMENTS

We thank B. Nickel for his support and valuable discussions. The work has been supported by DOE under Grant No. DE-FG02-93ER45503.

[1] C. D. Dimitrakopoulos, P. R. L. Malenfant, Adv. Mater. (Weinheim, Ger.) **14**, 99 (2002), and references therein.
[2] S. R. Forrest, Chem. Rev. (Washington, D.C.) **97**, 1793 (1997), and references therein.
[3] Y. Y. Lin, D. J. Gundlach, S. Nelson, and T. N. Jackson, IEEE Electron Device Lett. **18**, 87 (1997).
[4] I. Kymissis, C. D. Dimitrakopulos, and S. Purushothaman, IEEE Trans. Electron Devices **48**, 1060 (2001).
[5] S. Pratontep *et al.*, Synth. Met. **146**, 387 (2004).
[6] I. Yagi, K. Tsukagoshi, and Y. Aoyagi, Thin Solid Films **467**, 168 (2004).
[7] F. J. Meyer zu Heringdorf, M. C. Reuter, and R. M. Tromp, Nature (London) **412**, 517 (2001).
[8] R. Ruiz, B. Nickel, N. Koch, L. C. Feldman, R. F. Haglund, A. Kahn, and G. Scoles, Phys. Rev. B **67**, 125406 (2003).
[9] C. B. France *et al.*, Langmuir **19**, 1274 (2003).
[10] S. Lukas, G. Witte, and Ch. Woll, Phys. Rev. Lett. **88**, 028301 (2002).
[11] S. Lukas *et al.*, J. Chem. Phys. **114**, 10123 (2001).
[12] Y. L. Wang, W. Ji, D. X. Shi, S. X. Du, C. Saidel, Y. G. Ma, H. J. Gao, L. F. Chi, and H. Fuchs, Phys. Rev. B **69**, 075408 (2004).
[13] L. Chkoda *et al.*, Chem. Phys. Lett. **371**, 548 (2003).
[14] B. Krause *et al.*, J. Chem. Phys. **119**, 3429 (2003).
[15] E. Umbach and R. Fink, in *Organic Nanostructures: Science and Applications*, Proccedings of the International School of Physics "Enrico Fermi," Bologna, 2002, edited by V. M. Agronovich and G. C. La Rocca (IOS Press, Amsterdam, 2002), p. 233.
[16] S. Sohnchen, S. Lukas, and G. Witte, J. Chem. Phys. **121**, 525 (2004).
[17] S. Lukas *et al.*, ChemPhysChem **5**, 266 (2004).
[18] G. Beernink *et al.*, Appl. Phys. Lett. **85**, 398 (2004).
[19] J. H. Kang and X.-Y. Zhua, Appl. Phys. Lett. **82**, 3248 (2003).
[20] Ph. Guaino *et al.*, Surf. Sci. **540**, 107 (2003).
[21] Ph. Guaino *et al.*, Appl. Surf. Sci. **212-213**, 537 (2003).
[22] C. Baldacchini *et al.*, Surf. Sci. **566-568**, 613 (2004).
[23] L. Gavioli *et al.*, Surf. Sci. **566**, 624 (2004).
[24] A. Langner, Surf. Sci. **574**, 153 (2005).
[25] E. C. Sanchez and S. J. Sibener, J. Phys. Chem. B **106**, 8019 (2002).
[26] R. Malik *et al.*, J. Cryst. Growth **150**, 984 (1995).
[27] D. Eres *et al.*, Appl. Phys. Lett. **55**, 1008 (1989).
[28] S. Iannotta *et al.*, Appl. Phys. Lett. **76**, 1845 (2000).
[29] S. Iannotta *et al.*, Synth. Met. **122**, 221 (2001).
[30] L. Casalis, M. F. Danisman, B. Nickel, G. Bracco, T. Toccoli, S. Iannotta, and G. Scoles, Phys. Rev. Lett. **90**, 206101 (2003).
[31] K. Glockler *et al.*, Surf. Sci. **405**, 1 (1998).
[32] K. Walzer *et al.*, Surf. Sci. **573**, 346 (2004).
[33] V. Oja and E. M. Suuberg, J. Chem. Eng. Data **43**, 486 (1998).
[34] This seeding ration is estimated by determining the pentacene flux at the nozzle from the monolayer completion time and comparing this value to the helium flux.
[35] D. Miller, in *Atomic and Molecular Beam Methods*, edited by G. Scoles (Oxford University Press, New York, 1988), Vol. 1, p. 14.
[36] M. F. Danisman *et al.*, J. Phys. Chem. B **106**, 11771 (2002).
[37] G. Comsa, in *Atomic and Molecular Beam Methods*, edited by G. Scoles (Oxford University Press, New York, 1992), Vol. 2, p. 463.
[38] J. J. de Miguel *et al.*, Surf. Sci. **189/190**, 1062 (1987).
[39] Actually previously we assumed a sixfold periodicity in Ref. 30; however, the sharper peaks observed on the flat surface suggest that the periodicity is in fact 6.1.
[40] R. Campbell, J. Robertson, and J. Trotter, Acta Crystallogr. **14**, 705 (1961).
[41] D. Farias (Private communication).
[42] M. Eremtchenko *et al.* (unpublished).
[43] W. F. Egelhoff, Jr. and I. Jacob, Phys. Rev. Lett. **62**, 921 (1989).
[44] R. Kunkel, B. Poelsema, L. K. Verneij, and G. Cosma, Phys. Rev. Lett. **65**, 733 (1990).
[45] A. C. Durr, F. Schreibar, K. A. Ritley, V. Kruppa, J. Krug, H. Dosch, and B. Struth, Phys. Rev. Lett. **90**, 016104 (2003).